Research Article
Sciences of Pharmacy

Griess Assay Evaluation of Nitric Oxide Scavenging by a Multi-Extract Emulgel for Topical Steroid Withdrawal

Wahyu Bachtiar, **Tyssa Mariyana**, **Nurul Hidayatri**, **Bheta Sari Dewi**, **Ayu Werawati**

[The author informations are in the declarations section. This article is published by ETFLIN in Sciences of Pharmacy, Volume 5, Issue 4, 2026, Page 410-425. DOI: 10.58920/sciphar0504785]

Received
23 August 2026

Revised
02 October 2026

Accepted
25 October 2026

Published
01 November 2026

Editor
Garnadi Jafar

Keywords: Andrographis paniculata, Tinospora cordifolia, Curcuma longa, Piper nigrum, emulgel formulation, topical steroid withdrawal.

CC BY 4.0

AUTHOR (2026)

Abstract: Topical steroid withdrawal (TSW) is an iatrogenic dermatosis following prolonged topical corticosteroid use, with limited non-steroidal alternatives. This study developed a multi-extract emulgel containing *Andrographis paniculata*, *Tinospora cordifolia*, *Curcuma longa*, and *Piper nigrum* and screened its nitric oxide (NO)-scavenging activity. Standardized ethanolic extracts were incorporated into eight emulgels (F1–F8) using a 2^3 full factorial design, varying *A. paniculata* (3–5%), *T. cordifolia* (4–6%), and *C. longa* (4–6%) with *P. nigrum* fixed at 10%. Physical characterization showed homogeneous oil-in-water emulgels with pH 5.26–5.90, spreadability 6.7–6.8 cm, and viscosity 12,560–17,120 cP. IC_{50} values for all formulations exceeded the highest tested concentration (100 µg/mL) without reaching the concentration-response curve plateau, and are reported as > 100 µg/mL compared to 18.48 µg/mL for ascorbic acid. Descriptive ranking placed F4 first, followed by F7 and F8. Exploratory factorial analysis indicated that *C. longa* levels and the *A. paniculata* × *T. cordifolia* interaction drove IC_{50} variation, showing that higher extract loading did not enhance activity. Because this cell-free assay reflects only direct chemical NO scavenging, findings are strictly preliminary and descriptive. Future validation requires independent runs across an expanded concentration range capturing the full upper plateau. F4 is tentatively proposed as the lead formulation for confirmatory testing and subsequent stability, cell-based, and in vivo studies.

Introduction

Topical corticosteroids (TCSs) remain the standard first-line treatment for atopic dermatitis (AD), yet their pattern of use carries a significant risk. Prolonged and unsupervised application of medium- to high-potency TCSs is frequently reported, and this behaviour contributes to the emergence of topical steroid withdrawal (TSW), also known as red skin syndrome or topical steroid addiction (1). TSW is an increasingly recognised, and still medically contested, dermatosis characterized by diffuse erythema, a burning sensation, extreme pruritus and prolonged sleep disturbance following the discontinuation of TCSs after prolonged use (2). An evidence gap map that analysed the international literature and patient community platforms confirmed that TSW is a distinct adverse effect of prolonged TCS use, while also highlighting the scarcity of high-quality mechanistic and interventional research (3). Patient-reported studies further indicate a protracted disease course and a severe impact on quality of life, comparable to or worse than that of other chronic inflammatory skin diseases (4).

Natural products have attracted considerable interest as potential sources of bioactive compounds for topical applications. *Andrographis paniculata*, *Tinospora cordifolia*, *Curcuma longa*, and *Piper nigrum* contain various phytoconstituents that have been reported to possess antioxidant and inflammation-related biological activities (5). Combining plant extracts with complementary phytochemical profiles may provide a broader biological effect than the use of a single extract (6). Nevertheless, the biological activity of a combination should be experimentally evaluated because interactions among extracts may influence the overall activity of the formulation (7). *A. paniculata* contains andrographolide, a major diterpenoid lactone that has been reported to modulate inflammation-related signaling and reduce the expression of inflammatory mediators, including inducible nitric oxide synthase (iNOS) and cyclooxygenase-2 (COX-2) (8). Ethanol extracts of *A. paniculata* have also demonstrated anti-inflammatory activity in experimental models (9). *T. cordifolia* is a medicinal plant containing alkaloids, diterpenoid lactones, glycosides, steroids, and other bioactive constituents and has been reported to possess antioxidant, immunomodulatory, and inflammation-related activities (10). Its constituents have also been reported to modulate the MAPK pathway and

the NLRP3 inflammasome, and pre-incubation of lipopolysaccharide (LPS)-stimulated macrophages with *T. cordifolia* extract significantly reduced prostaglandin E2 (PGE2) synthesis, an effect associated with decreased cyclooxygenase-2 (COX-2) expression (11). *C. longa*, particularly its curcuminoid constituents, has been widely investigated for anti-inflammatory and redox-regulating properties and has been associated with modulation of iNOS-related processes and reactive nitrogen species (12). In addition, *C. longa* preparations have demonstrated anti-inflammatory effects in experimental topical models (12). *P. nigrum*, particularly its major constituent piperine, may function as a bio-enhancer and potentially improve the bioavailability or topical delivery of co-administered phytoconstituents. Black pepper extract has also been investigated for its ability to enhance the penetration of turmeric-derived constituents in topical delivery systems (13). Collectively, these findings provide a rationale for investigating the four botanicals as a multi-extract system; however, their combined effects on NO-scavenging activity have not been directly established.

Nitric oxide (NO) is an important signaling molecule involved in various physiological and pathological processes in the skin, including epidermal barrier homeostasis, wound healing, immune responses, and inflammation (14). Under inflammatory conditions, altered NO production and the activity of nitric oxide synthases, particularly inducible nitric oxide synthase (iNOS), may contribute to inflammatory and oxidative/nitrosative processes in the skin (15). Therefore, the ability of a test sample to scavenge NO has been investigated as a preliminary indicator of its potential to modulate NO-related oxidative and inflammatory processes. The Griess assay provides a simple and widely used in vitro approach for indirectly assessing NO production or scavenging activity through the measurement of nitrite, a relatively stable oxidation product of NO (16). However, NO scavenging activity determined using this assay should be interpreted as preliminary evidence of NO-related antioxidant activity and does not, by itself, establish a specific anti-inflammatory effect or the underlying molecular mechanism of action (17).

An emulgel is a semisolid topical delivery system that combines the characteristics of an emulsion and a gel. This dosage form can provide practical advantages for topical application, including ease of spreading, acceptable skin characteristics, and the ability to incorporate both hydrophilic and lipophilic components (18, 19). These characteristics make an emulgel a potentially suitable delivery platform for a combination of plant extracts with diverse physicochemical properties (20). Therefore, incorporation of multiple botanical extracts into an emulgel may provide a practical formulation strategy for topical delivery, while its biological activity requires experimental evaluation.

Our previous study investigated a spray-gel formulation containing the same four Indonesian medicinal plant extracts, namely *A. paniculata*, *T. cordifolia*, *C. longa*, and *P. nigrum*, for potential application in topical steroid withdrawal. Building on this preliminary formulation work, the present study explores a different topical delivery platform and a more systematic formulation optimization strategy (11). Specifically, an emulgel system was developed to provide both hydrophilic and lipophilic characteristics, potentially facilitating the incorporation and topical delivery of diverse bioactive constituents (21). In addition, a 2^3 full factorial design generated in Design-Expert® software was employed to systematically investigate the effects and interactions of formulation variables across eight formulations rather than evaluating a single fixed formulation (3, 22).

Despite increasing interest in herbal formulations for inflammatory skin conditions, many studies have focused on general antioxidant or anti-inflammatory activities rather than specifically evaluating NO-related activity in the context of TSW-associated inflammatory manifestations (3). Previous studies have also commonly investigated single-plant extracts or empirically selected combinations, whereas the present study employs a four-botanical combination based on the complementary pharmacological potential of the selected extracts. Thus, the research gap addressed in this study is not the absence of herbal combinations, but the limited availability of systematically optimized multi-extract topical formulations that are developed using factorial design and preliminarily evaluated for NO-scavenging activity in the context of TSW (23).

In the present study, the sodium nitroprusside (SNP)–Griess assay was used to evaluate the NO-scavenging activity of the formulated emulgels. This cell-free assay evaluates the ability of the formulations to reduce NO-derived nitrite generated from sodium nitroprusside and therefore reflects direct NO-scavenging potential rather than inhibition of cellular NO production or direct inhibition of iNOS activity (24). Because the reaction mixture contains neither cells nor NO synthase, any reduction in nitrite can arise only from direct chemical interaction of sample constituents with NO or NO-derived reactive nitrogen species. The quantitative evaluation of NO-scavenging activity, including IC_{50} determination, was therefore used as a preliminary biological screening endpoint rather than as direct evidence of a specific anti-inflammatory mechanism (25).

Based on the reported activities of the individual botanicals, we hypothesized that their combination may provide complementary NO-scavenging and inflammation-related activity. However, the proposed interactions among the four botanicals represent a mechanistic hypothesis and were not directly investigated in the present study. Accordingly, the current work focuses on formulation development, physicochemical characterization, and preliminary evaluation of NO-scavenging activity, while confirmation of specific inflammatory pathways, including NF-κB, MAPK, NLRP3, and iNOS-related mechanisms, requires further cell-based and molecular investigations (26).

This study therefore aimed to formulate a multi-extract emulgel containing *A. paniculata*, *T. cordifolia*, *C. longa*, and *P. nigrum* using a 2^3 full factorial design, to characterize the physical properties of the resulting formulations, and to evaluate their NO-scavenging activity using the SNP–Griess assay as a preliminary screening endpoint. The study further aimed to identify a lead formulation for subsequent cell-based and mechanistic evaluation relevant to inflammatory manifestations

associated with TSW.

The novelty of the present work lies in three aspects. First, to the best of our knowledge, this is the first report of an emulgel combining *A. paniculata*, *T. cordifolia*, *C. longa*, and *P. nigrum*, botanicals widely used in Indonesian traditional medicine, developed specifically as a non-steroidal topical candidate for inflammatory manifestations associated with topical steroid withdrawal. Second, instead of testing a single empirically fixed combination, the levels of the three active extracts were varied systematically using a 2^3 full factorial design, so that their main and interaction effects on nitric oxide-scavenging potency could be quantified. Third, the extracts were standardized for non-specific quality parameters and for their principal marker compounds before formulation, linking formulation composition to a defined chemical baseline. The preliminary results also suggest that, within the studied range, increasing extract loading did not increase nitric oxide-scavenging potency, which is relevant for the rational design of multi-extract topical products, although this observation requires confirmation in independent assay runs.

Methodology

Materials

The plant materials used were the dried herb of *A. paniculata* (sambiloto), the stem of *T. cordifolia* (brotowali), the rhizome of *C. longa* (kunyit) and the fruit of *P. nigrum* (black pepper). The plant materials were obtained from Lansida supplier, Special Region of Yogyakarta, Indonesia, in June 2025 and were authenticated at Materia Medica Herbal Laboratory, Batu, East Java, Indonesia (authentication numbers 186/LH/06/25 to 189/LH/06/25). The chemicals and excipients used were 96% ethanol (Merck, Germany), distilled water, Carbopol® 940 (Lubrizol, USA), triethanolamine (Merck, Germany), propylene glycol (Merck, Germany), DMDM hydantoin (Ashland, USA), liquid paraffin (Merck, Germany), Span 80 (Merck, Germany), Tween 80 (Merck, Germany), methylene blue (Merck, Germany), sodium nitroprusside (Sigma-Aldrich, USA), phosphate-buffered saline (Gibco, USA), Griess reagents A and B (Sigma-Aldrich, USA), and ascorbic acid (Sigma-Aldrich, USA). The principal instruments included a rotary vacuum evaporator (Büchi [Rotavapor R-300], Switzerland), Soxhlet extraction apparatus (Pyrex, USA), analytical balance (Mettler Toledo [XPR305DR], Switzerland), ultrasonic bath (Elma Elmasonic [P 70 H], Germany), centrifuge (Hettich [ROTOFIX 32], Germany), vortex mixer (IKA [Vortex 3], Germany), incubator (Memmert [IN55], Germany), digital pH meter ([Lutron pH Meter]), UV–Vis spectrophotometer ([GENESYS 180, Thermo Scientific, USA]), Brookfield viscometer (AMETEK Brookfield [DV2T], AMETEK Brookfield, USA), and UV–Vis microplate reader (BioTek [BioTek Synergy H1], USA). The experimental design and factorial analysis were performed using Design-Expert® version 13 (Stat-Ease Inc., Minneapolis, MN, USA), and nonlinear concentration–response fitting was performed using GraphPad Prism version 10 (GraphPad Software, San Diego, CA, USA).

Sample Preparation and Extraction

Fresh plant materials were authenticated, cleaned, cut into small pieces and dried away from direct sunlight before being milled into a coarse powder. The dried herb of *A. paniculata* and the stem of *T. cordifolia* were milled and each macerated (500 g) in 96% ethanol at a 1:10 ratio for three days, after which the filtrate was collected through filter paper. The rhizome of *C. longa* (500 g) and the fruit of *P. nigrum* (500 g) were extracted separately by Soxhlet extraction using 96% ethanol at a 1:10 ratio until the siphoned solvent ran clear. Each filtrate was concentrated using a rotary vacuum evaporator at 30–40 °C to obtain a thick extract, which was stored at low temperature. An ethanol-free test was performed by esterification (adding concentrated sulphuric acid and acetic acid followed by heating); the absence of the characteristic ethyl-acetate odour indicated an ethanol-free extract (11).

Physicochemical and Phytochemical Standardization

Moisture content, total ash, and acid-insoluble ash were determined according to standard pharmacopoeial procedures. Moisture content was determined by drying approximately 2 g of powdered plant material at 105 ± 2 °C to constant weight and expressed as a percentage of weight loss. Total ash was determined by incinerating approximately 2 g of the sample in a crucible at approximately 600 °C until constant weight, and the residue was expressed as a percentage of the initial sample weight. Acid-insoluble ash was determined by treating the total ash with 3 N hydrochloric acid, filtering the insoluble residue, washing it with hot distilled water, and igniting it to constant weight; the result was expressed as a percentage of the initial sample weight. Qualitative phytochemical screening was performed using standard chemical tests to detect alkaloids, flavonoids, phenolics, tannins, saponins, terpenoids, steroids, and glycosides based on characteristic color changes, precipitate formation, or persistent foam (27).

Quantitative Determination of Curcumin, Piperine, and Andrographolide

Curcumin, piperine, and andrographolide contents were estimated separately in the extracts of *C. longa*, *P. nigrum*, and *A. paniculata*, respectively, using UV–Visible spectrophotometry. Methanol of analytical grade was used as the solvent for the preparation of reference-standard solutions, sample solutions, and blank measurements. The marker compounds were analyzed separately to minimize spectral interference from other extract constituents (28).

Curcumin reference standard was dissolved in methanol and scanned over the wavelength range of 350–500 nm. The wavelength of maximum absorption was determined at approximately 421–422 nm and was used for the analysis of the *C. longa* extract. A curcumin calibration curve was prepared using standard working solutions at concentrations of 1, 2, 3, 4, 5, and 6 µg/mL in methanol. The absorbance was measured at 421–422 nm against methanol as the blank. Curcumin content was calculated from the linear regression equation of the calibration curve (28).

Piperine reference standard was dissolved in methanol and scanned over 250–400 nm. The maximum absorption wavelength was determined at approximately 331 nm and used to analyze the *P. nigrum* extract. Standard working solutions of piperine (2, 4, 6, 8, 10, and

Table 1. Independent variables and coded levels used in the 2^3 factorial design.

Independent variable	Symbol	Function in formulation	Low level (−1)	High level (+1)
Factor A: [*A. paniculata*]	X1	[active extract]	3%	5%
Factor B: [*T. cordifolia*]	X2	[active extract]	4%	6%
Factor C: [*C. longa*]	X3	[active extract]	4%	6%

Table 2. Experimental matrix of the 2^3 full factorial design.

Formulation	X1	X2	X3	A (%)	T (%)	C (%)
F1	−1	−1	+1	3	4	6
F2	+1	+1	+1	5	6	6
F3	−1	+1	+1	3	6	6
F4	−1	−1	−1	3	4	4
F5	+1	−1	+1	5	4	6
F6	+1	−1	−1	5	4	4
F7	+1	+1	−1	5	6	4
F8	−1	+1	−1	3	6	4

Table 3. Composition of the multi-extract emulgel formulas (% w/w).

Ingredient	Function	F1	F3	F3	F4	F5	F6	F7	F8
A. paniculata extract	Active Ingredient	3	5	3	3	5	5	5	3
T. cordifolia extract	Active Ingredient	4	6	6	4	4	4	6	6
C. longa extract	Active Ingredient	6	6	6	4	6	4	4	4
P. nigrum extract	Bio-enhancer	10	10	10	10	10	10	10	10
Carbopol 940	Gelling agent	1	1	1	1	1	1	1	1
TEA	pH adjuster	1	1	1	1	1	1	1	1
Propylene glycol	Humectant	10	10	10	10	10	10	10	10
DMDM hydantoin	Preservative	0.6	0.6	0.6	0.6	0.6	0.6	0.6	0.6
Liquid paraffin	Emollient	10	10	10	10	10	10	10	10
Span 80	Emulsifier	1.4	1.4	1.4	1.4	1.4	1.4	1.4	1.4
Tween 80	Emulsifier	3.6	3.6	3.6	3.6	3.6	3.6	3.6	3.6
Distilled water	Solvent	ad 100	ad 100	ad 100	ad 100	ad 100	ad 100	ad 100	ad 100

12 µg/mL) were prepared in methanol. Absorbance was measured at 331 nm against methanol as a blank, and piperine content was calculated from the standard calibration curve (29).

Andrographolide reference standard was dissolved in methanol and scanned over 200–400 nm. The maximum absorption wavelength was determined at approximately 224 nm and used to analyze the *A. paniculata* extract. A calibration curve was prepared from andrographolide standard working solutions at concentrations of 5, 10, 15, 20, 25, and 30 µg/mL in methanol. The sample absorbance was measured at 224 nm against methanol as the blank, and the andrographolide content was calculated from the corresponding calibration equation (30).

Briefly, 100 mg of extract in 10 mL methanol was sonicated (15 min), filtered (0.45 µm), diluted as needed, and measured in triplicate. Marker content (mg/g) was calculated from the calibration curve (30).

Factorial Experimental Design

Eight emulgel formulas were prepared using a 2^3 full factorial design generated in Design-Expert® version 13 (Stat-Ease Inc., Minneapolis, MN, USA) in which the extract concentrations were varied while the base excipients were kept constant (**Table 1**). The factorial design was used to estimate the direction and relative magnitude of the main and interaction effects of the *A. paniculata*, *T. cordifolia*, and *C. longa* extract levels on NO-scavenging potency (IC_{50}) and to guide the selection of a lead formulation, rather than to test formal statistical hypotheses. Because each formulation was evaluated once (unreplicated design), IC_{50} was $\log_{10}$-transformed to stabilize variance, and the factorial effects were estimated using the coded polynomial model shown in Equation (1). Potentially active effects were screened using a half-normal probability plot and Lenth's pseudo-standard-error method ($\alpha = 0.05$), and the results were interpreted as exploratory (22). The mathematical relationship between the formulation variables and the response was evaluated using the coded polynomial model presented in **Equation 1**, where β_0 is the intercept; β_1, β_2, and β_3 are the main-effect coefficients; β_{12}, β_{13}, β_{23}, and β_{123} are the interaction coefficients; and X_1, X_2, and X_3 are the coded levels (−1 or +1) of the *A. paniculata*, *T. cordifolia*, and *C. longa* extracts, respectively. In the present study, *P. nigrum* extract was maintained at a constant concentration and was therefore not included as an independent variable in the Design-Expert experimental design. The complete combination of factor levels for each emulgel formulation is presented in **Table 2**.

$$\log_{10}(\mathrm{IC}_{50}) = \beta_0 + \beta_1 X_1 + \beta_2 X_2 + \beta_3 X_3 + \beta_{12} X_1 X_2 + \beta_{13} X_1 X_3 + \beta_{23} X_2 X_3 \beta_{123} X_1 X_2 X_3 \quad \textbf{(Eq. 1)}$$

Emulgel Formulation

The aqueous phase was prepared by dispersing Carbopol 940 in distilled water and allowing it to swell, followed by the addition of propylene glycol and DMDM hydantoin. The oil phase was prepared by mixing liquid paraffin with Span 80, while Tween 80 was incorporated into the aqueous phase to form a stable emulsion system. The oil phase was then added slowly to the aqueous phase under continuous stirring, and TEA was added gradually to neutralise the Carbopol and form the gel consistency. The *A. paniculata*, *T. cordifolia* and *C. longa* extracts were incorporated as active substances, followed by the *P. nigrum* extract as a bio-enhancer, and the preparation was made up to the final weight with distilled water and homogenised (31). The vehicle composition (liquid paraffin oil phase, Span 80–Tween 80 emulsifier pair, and Carbopol 940 gel base) was based on the cited emulgel formula and kept identical in all formulations; therefore, phase-behaviour optimization of the vehicle (e.g., construction of a ternary phase diagram) was outside the scope of this study, and only the extract levels were varied. The detailed concentrations and proportions of active ingredients and excipients used in each of the eight emulgel formulations (F1–F8) are presented in **Table 3**.

Physical Evaluation

The prepared emulgel formulations were evaluated for their physical and physicochemical properties, including organoleptic characteristics, homogeneity, emulsion type, pH, adhesion, spreadability, and viscosity. Organoleptic properties were evaluated by direct visual and sensory observation of the colour, odour, and consistency of each formulation. Homogeneity was assessed by visual examination of the emulgel after spreading a small amount of the formulation on a glass slide to ensure uniform distribution of the components and the absence of visible particles, lumps, or aggregates. The emulsion type was determined using the methylene blue dye test. A small amount of each emulgel was spread on a glass slide, one drop of methylene blue solution was added, and the preparation was observed under a light microscope at [4×] magnification. Rapid and uniform diffusion of the water-soluble dye throughout the continuous phase, with unstained dispersed droplets, was taken as the indicator of an oil-in-water (O/W) emulsion, whereas retention of the dye as discrete blue spots would indicate a water-in-oil (W/O) emulsion. The pH was measured using a calibrated digital pH meter by dispersing the emulgel in distilled water and allowing the sample to equilibrate before measurement. The measured pH was compared with the generally acceptable skin pH range of approximately 4.5–6.5. Spreadability was evaluated by placing 0.5 g of emulgel between two glass plates and applying a 1000 g load for 1 min. The diameter of the spread formulation was then measured, with a spreadability range of approximately 5–7 cm considered desirable for topical application. Adhesion was evaluated by placing a defined amount of emulgel between two glass slides, applying an 80 g load, and measuring the time required for the slides to separate. An adhesion time of more than 1 s was considered acceptable for topical preparations. Viscosity was determined using a Brookfield rotational viscometer at controlled room temperature using an appropriate spindle and rotational speed. The viscosity value was recorded in centipoise (cP). The pH, spreadability, adhesion, and viscosity measurements were performed in triplicate (n = 3) for each formulation. A viscosity range of approximately 6,000–50,000 cP was used as a practical reference for evaluating the consistency and spreadability of the semisolid emulgel formulations (32).

Emulgel Sample Preparation For The Griess Assay

A 100-mg portion of each emulgel formulation (F1–F8) was dispersed in 10 mL phosphate-buffered saline (PBS), vortexed, and sonicated for 15–30 min to facilitate the release of the incorporated extracts. The samples were then centrifuged and the supernatants were collected and filtered. The resulting stock solutions were serially diluted with PBS to obtain concentrations of 20, 40, 60, 80, and 100 µg/mL, calculated based on the total combined extract content of each formulation. The prepared samples were subsequently evaluated using the Griess assay (33).

Nitric Oxide Scavenging Assay (Griess Method)

Nitric oxide scavenging was determined using the Griess method. Briefly, a 5 µL sample was mixed with 10 mM sodium nitroprusside (SNP) in PBS and incubated at room temperature for 150 minutes. Griess reagent B (100 µL) was then added and the mixture left for 5 minutes, followed by Griess reagent A (100 µL) and a further 30-minute incubation at room temperature. Absorbance was read at 540 nm using a microplate reader, and ascorbic acid was used as the positive control (34)(35).

Data Analysis

Results are presented as figures and tables. The percentage of NO scavenging was calculated for each concentration using **Equation 2**, where $A_{control}$ = absorbance of the control, A_{sample} = absorbance of the sample + reaction system and A_{blank} = absorbance of the sample/formulation blank without the NO-generating reaction.

IC_{50} was defined as the sample concentration producing 50% scavenging of nitric oxide generated by sodium nitroprusside under the stated assay conditions, rather than as a measure of biological inhibition, and was estimated by nonlinear regression using a four-parameter logistic (4PL, variable-slope) model. When the estimated IC_{50} exceeded the highest tested concentration (100 µg/mL), it was reported as > 100 µg/mL. The corresponding numerical values obtained by extrapolating the fitted curves beyond the tested range are presented only as apparent estimates for descriptive ranking and for the exploratory factorial analysis, and they were not interpreted as reliable measures of potency.

Each formulation and concentration was measured in duplicate technical wells within a single assay run. Results are presented as mean ± standard deviation of duplicate

$$\text{NO scavenging } (\%) = \frac{A_{\text{control}} - (A_{\text{sample}} - A_{\text{blank}})}{A_{\text{control}}} \times 100 \quad \textbf{(Eq. 2)}$$

technical measurements. The duplicate wells were used to assess intra-assay precision and were averaged for calculation of percentage nitric oxide scavenging and apparent IC_{50} values. Because independent assay runs were not performed, no inferential comparisons between formulations (ANOVA, multiple comparisons, or significance testing) were conducted. The 95% confidence intervals reported for IC_{50} were derived from the curve fit of the mean responses and therefore reflect fitting uncertainty only, not between-run variability. Accordingly, all NO-scavenging results reported here are strictly preliminary and descriptive, and their validation requires independent assay runs performed on at least three separate occasions. Physical characterization data are presented as mean ± SD of three (n = 3) replicate measurements.

Results and Discussion

Extraction Method

The extraction yields ranged from 12.0% to 18.8% (**Table 4**). The highest yield was obtained from *C. longa* L. extracted by maceration (18.8%), whereas the lowest yield was observed for *T. cordifolia* (Willd.) Miers extracted by maceration (12.0%). The yield obtained for *T. cordifolia* was comparable to a previously reported cold-maceration yield of approximately 13.44%, although other studies have reported values ranging from 4.8% to 20.35%, depending on the solvent and extraction conditions. The yield of *C. longa* in the present study was higher than the 7.62% reported for cold maceration but lower than the 10.27% obtained using Soxhlet extraction in another study, indicating that solvent composition, solvent-to-material ratio, extraction time, temperature, and plant material characteristics strongly affect the final yield. Overall, the yields obtained in this study were within the range reported in the literature.

The physicochemical analysis showed moisture contents of 5.76–9.08%, total ash values of 2.12–4.24%, and acid-insoluble ash values of 0.03–0.56% (**Table 5**). *A. paniculata* exhibited the highest moisture content, whereas *C. longa* showed the highest total and acid-insoluble ash values. These findings were generally comparable with recent reports for medicinal plant materials, although differences may result from variations in plant part, geographical origin, drying conditions, and inorganic contamination. The low acid-insoluble ash values suggest minimal contamination with soil or sand and support the acceptable preliminary quality of the tested materials.

Qualitative phytochemical screening revealed the presence of alkaloids, flavonoids, phenolic compounds, and tannins in all four plant extracts (**Table 6**). Saponins were detected in *T. cordifolia* and *A. paniculata* , whereas steroids/triterpenoids were detected in *T. cordifolia*, *P. nigrum*, and *A. paniculata*. These findings are generally consistent with recent reports describing the occurrence of alkaloids, flavonoids, phenolics, steroids, and terpenoids in *T. cordifolia* and phenolic and terpenoid constituents in *A. paniculata*. The differences in phytochemical profiles may be related to plant species, plant part, geographical origin, solvent polarity, extraction method, and seasonal variation. Because the tests were qualitative, the results indicate the presence or absence of phytochemical groups and should not be interpreted as differences in their concentrations.

Quantitative analysis showed that the *A. paniculata* extract contained the highest marker-compound level, with an andrographolide content of 2.4 mg/g extract, followed by curcumin in the *C. longa* extract at 1.6 mg/g extract and piperine in the *P. nigrum* extract at 1.1 mg/g

Table 4. Plant materials, botanical authentication numbers, extraction methods, extract weights, and extraction yields.

Plant material	Scientific Name	Botanical Authentication Numbers	Method	Extract (g)	Yield Extraction (%)
Brotowali	*T. cordifolia* (Willd.) Miers	187/LH/06/25	Maceration	60	12
Kunyit	*C. longa* L.	186/LH/06/25	Soxhlet	94	18.8
Lada hitam	*P. nigrum* L.	189/LH/06/25	Soxhlet	84	16.8
Sambiloto	*A. paniculata* (Burm.f.) Nees	188/LH/06/25	Maceration	82	16.4

Table 5. Non-specific quality parameters of the four plant extracts according to the Indonesian Herbal Pharmacopoeia.

Quality Control	*T. cordifolia*	*C. longa*	*P. nigrum*	*A. paniculata*	FHI Acceptance Criteria
Moisture content (%)	5.76	6.91	7.6	9.08	≤ 10%
Total ash content (%)	3.24	4.24	3.83	2.12	≤ 5%
Acid-insoluble ash (%)	0.26	0.56	0.45	0.03	≤ 1%

Table 6. Qualitative phytochemical screening of the plant extracts.

Phytochemical group	Qualitative test	*T. cordifolia*	*C. longa*	*P. nigrum*	*A. paniculata*
Alkaloids	Dragendorff's test	+	+	+	+
Flavonoids	Shinoda test	+	+	+	+
Phenolic compounds	Ferric chloride test	+	+	+	+
Tannins	Gelatin test	+	+	+	+
Saponins	Froth test	+	-	-	+
Steroids/triterpenoids	Liebermann–Burchard test	+	-	+	+

Note: (+) Presence; (−) Absence of the respective phytochemical group.

extract (**Table 7**). These results confirm the presence of the selected marker compounds in the respective extracts and provide preliminary information regarding their chemical composition. Curcumin was measured at 421 nm, piperine at 331 nm, and andrographolide at 224 nm. However, because the analysis was performed using UV–Visible

Table 7. Preliminary UV–Visible spectrophotometric quantification of selected marker compounds in plant extracts (mean ± SD, n = 3).

Sample Name	Marker Compound	Result	Unit	Method
C. longa extract	Curcumin	1.60 ± 0.0057	mg/g	Spectro 421 nm
P. nigrum extract	Piperine	1.13 ± 0.015	mg/g	Spectro 331 nm
A.paniculata extract	Andrographolide	2.39 ± 0.01	mg/g	Spectro 224 nm



Figure 1. Appearance of the emulgel formulations (F1–F8).

Table 8. Organoleptic test results of emulgel formulas.

Sample	Shape	Color	Smell	Sensory
F1	Thick	Brownish olive green	Aromatic	Cooling sensation
F2	Thick	Bright yellowish green	Aromatic	Cooling sensation
F3	Thick	Yellowish olive green	Aromatic	Cooling sensation
F4	Thick	Pale yellowish green	Aromatic	Cooling sensation
F5	Thick	Yellowish green	Aromatic	Cooling sensation
F6	Thick	Dark olive green	Aromatic	Cooling sensation
F7	Thick	Olive green	Aromatic	Cooling sensation
F8	Thick	Pale yellow-green	Aromatic	Cooling sensation

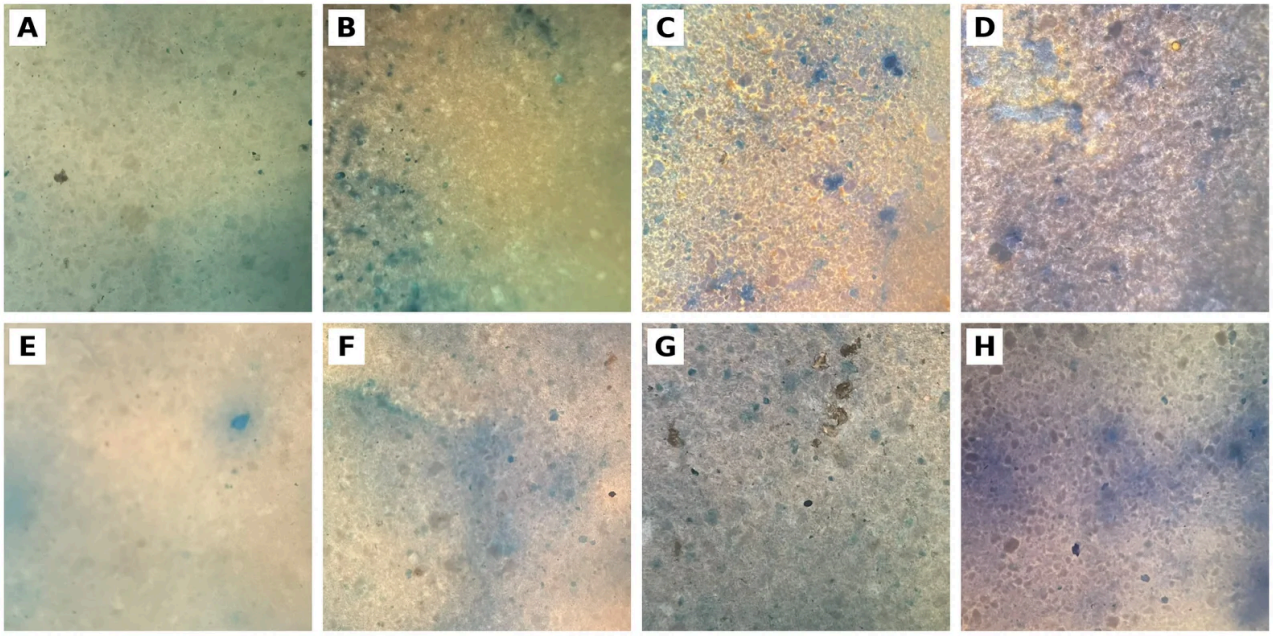


Figure 2. Methylene blue dye test of the emulgel formulations (F1–F8). Uniform distribution of the water-soluble dye in the continuous phase indicates an O/W emulsion. Panels A–H correspond to formulations F1–F8, respectively.

spectrophotometry, the results should be interpreted cautiously, particularly for complex plant extracts, because co-extractives may absorb at similar wavelengths.

Physical Evaluation of Emulgel

Organoleptic Characteristics

The organoleptic evaluation showed that all formulations (F1–F8) had a thick consistency and an aromatic odor. The color of the formulations varied from brownish olive green to dark olive green. Specifically, F1 was brownish olive green, F2 was bright yellowish green, F3 was yellowish olive green, F4 was pale yellowish green, F5 was yellowish green, F6 was dark olive green, F7 was olive green, and F8 was pale yellow-green (**Figure 1**). All formulations produced a cooling sensation upon application (**Table 8**). Overall, the formulations exhibited comparable physical characteristics, particularly in terms of consistency, odor, and sensory response. The observed variation in color may be associated with differences in the concentration or distribution of the extract and other formulation components.

Emulsion Type Evaluation

The emulsion type evaluation demonstrated that all formulations (F1–F8) were oil-in-water (O/W) emulsions, as indicated by the rapid and uniform diffusion of methylene blue throughout the continuous phase while the dispersed oil droplets remained unstained (**Figure 2**). This result indicates that the oil phase was dispersed as fine droplets within a continuous aqueous phase. Consequently, the formulations are expected to be readily dispersible or washable with water and to provide a light, non-greasy feel during topical application. The O/W emulsion type is considered appropriate for topical preparations because the external aqueous phase can promote a cooling sensation, improve user acceptability, and facilitate the release of hydrophilic active constituents. The consistent O/W characteristics observed across all formulations also suggest that the selected emulsifier system was effective in stabilizing the dispersion of the oil phase in the aqueous phase (36).

Homogeneity Test

The homogeneity test showed that all formulations (F1–F8) were homogeneous. No visible coarse particles, lumps, phase separation, or uneven distribution of components were observed during the examination. This finding indicates that the mixing process was effective and that the ingredients, including the active substances and excipients, were uniformly distributed throughout each formulation. The homogeneous appearance of all formulations is an important indicator of good physical quality, as it supports consistent product performance and helps ensure uniform application and dose distribution during topical use (37).

pH Test

The pH values of formulations F1–F8 ranged from 5.26 ± 0.01 to 5.90 ± 0.02. Formulation F1 showed the highest pH, whereas F8 showed the lowest pH. The low standard deviation values (0.01–0.06) indicate good repeatability of the pH measurements. All formulations exhibited a slightly acidic pH, which is generally considered suitable for topical application because it is close to the physiological acidity of the skin surface. Previous studies have reported that topical gels and creams commonly exhibit acceptable pH values within approximately 4.5–6.5, although the optimal range may depend on the intended application site, formulation components, and active ingredients. Therefore, the pH results suggest that all tested formulations may have acceptable preliminary skin compatibility. However, pH alone cannot establish dermatological safety, and further irritation, sensitization, and stability studies are required (38).

Adhesion Test

The adhesion test results of the emulgel formulations showed adhesion times ranging from 11 ± 1.00 to 16 ± 2.65 min (**Table 9**). Formulations F3 and F6 exhibited the shortest adhesion time, both at 11 min, whereas F5 and F8 showed the longest adhesion time of 16 min. The other formulations demonstrated intermediate adhesion times, namely 12 ± 1.00 min for F2 and F7, 13 ± 3.06 min for F4, and 14 ± 1.53 min for F1. These results indicate that all formulations were able to remain in contact with the surface for several minutes, which may support sufficient residence time during topical application. The differences in adhesion among formulations may be related to variations in the composition and concentration of the formulation components, particularly the gelling and emulsifying agents, which can influence the consistency and cohesive properties of the emulgel. Higher adhesion may be advantageous for topical preparations because prolonged contact with the skin can potentially increase the residence time of the active constituents at the application site. However, excessively high adhesion may reduce the ease of spreading and patient acceptability. Overall, the adhesion results indicate that the F1–F8 formulations possessed adequate adhesive properties for topical application (11).

Table 9. Adhesion test results of the emulgels (mean ± SD, n = 3).

Sample	Adhesion Time (min), Mean ± SD
F1	14 ± 1.53
F2	12 ± 1.00
F3	11 ± 1.00
F4	13 ± 3.06
F5	16 ± 1.00
F6	11 ± 1.53
F7	12 ± 1.00
F8	16 ± 2.65

Table 10. Spreadability test results of the emulgels (mean ± SD, n = 3).

Sample	Spreadability (cm), Mean ± SD
F1	6.8 ± 0.058
F2	6.7 ± 0.058
F3	6.8 ± 0.058
F4	6.8 ± 0.058
F5	6.8 ± 0.058
F6	6.8 ± 0.058
F7	6.7 ± 0.058
F8	6.7 ± 0.058

Table 11. Viscosity of the emulgel formulations (spindle 64, 30 rpm; mean ± SD, n = 3).

Sample	Viscosity (cP), Mean ± SD
F1	16.380 ± 86.60
F2	13.800 ± 43.59
F3	13.620 ± 26.46
F4	16.180 ± 20.00
F5	17.120 ± 36.06
F6	12.560 ± 26.46
F7	13.800 ± 62.45
F8	16.980 ± 43.59

Spreadability

The spreadability values of formulations F1–F8 ranged from 6.7 to 6.8 cm (**Table 10**). F1, F3, F4, F5, and F6 showed a spreadability of 6.8 ± 0.058 cm, whereas F2, F7, and F8 showed 6.7 ± 0.058 cm. The small difference among the formulations suggests that the tested formulation variables had only a limited effect on the spreading diameter under the applied test conditions. The low standard deviation indicates good repeatability of the measurements. Overall, the formulations exhibited acceptable spreading properties, which may facilitate uniform application to the skin. Values in the range of approximately 5–7 cm have been reported as suitable for topical gel application in comparable studies, although direct comparisons should be made cautiously because spreadability is highly method-dependent.

Viscosity Evaluation

The viscosity values of formulations F1–F8 ranged from 12,560 to 17,120 cP (**Table 11**). Formulation F5 exhibited the highest viscosity (17,120 ± 36.06 cP), whereas F6 showed the lowest value (12,560 ± 26.46 cP). The higher viscosity of F5 may provide greater structural consistency and prolonged retention on the application surface, although excessively viscous formulations may be more difficult to spread. In contrast, the lower viscosity of F6 may facilitate spreading but could reduce the formulation's resistance to flow and retention. All eight formulas fell within the 6,000–50,000 cP range specified for emulgel preparations under SNI 16-4399-1996, and none approached either boundary, indicating a comfortable formulation margin (39).

Nitric Oxide Scavenging

NO-scavenging activity was assessed using Griess reagent detection at 540 nm (40). The method rests on the spontaneous release of NO radicals by SNP in aqueous solution at physiological pH. The liberated NO reacts with dissolved oxygen to form nitrite ions, and it is this nitrite that is quantified colorimetrically through the Griess diazotisation reaction between nitrite, sulfanilamide and N-(1-naphthyl)ethylenediamine. Compounds capable of scavenging NO compete with oxygen and thereby reduce nitrite formation and lower absorbance (8). The decrease in absorbance relative to the negative control therefore represents the extent to which the test sample chemically scavenges NO and thereby limits nitrite accumulation (41).

Two control parameters attest to the validity of the assay system. A reagent blank absorbance of 0.0853 indicates a low and stable reagent background, while a negative control absorbance of 0.6120 ± 0.0001 demonstrates consistent NO release by SNP across wells. The dynamic range of 0.527 absorbance units between blank and negative control provides an adequate measurement window to resolve both partial and near-complete scavenging. All readings were taken on a single 96-well microplate, eliminating inter-plate variability as a source of systematic error.

Nonlinear concentration–response analysis using a four-parameter logistic model showed that the positive control had the lowest IC_{50} value (18.4836 µg/mL), indicating the highest apparent potency under the assay conditions. In contrast, the estimated IC_{50} values of all formulations exceeded the highest concentration tested (100 µg/mL); the IC_{50} of each formulation is therefore reported as > 100 µg/mL. The numerical values in **Table 12** were obtained by extrapolating the fitted curves beyond the experimental range and are presented only as apparent estimates for descriptive ranking: F4 had the lowest apparent IC_{50} (approximately 124 µg/mL), followed by F7 and F8 (approximately 157 and 159 µg/mL), whereas F6 had the highest (approximately 1,057 µg/mL). Estimates above approximately 600 µg/mL (F1, F2, F3, F5, and F6) lie six-fold or more beyond the tested range and carry no reliable quantitative meaning. The upper asymptotes of the unconstrained fits also exceeded 100% for all

Table 12. Nonlinear sigmoidal dose–response regression parameters and apparent (extrapolated) IC_{50} values of the formulations (4PL model, variable slope; n = 2 technical replicate wells per concentration, single assay run).

Sample	Extract loading (A/T / C, %)	Apparent IC_{50} (µg/mL)[a]	R^2	pIC50	95% CI	Hill slope	Bottom	Top
Positive Control	-	18.4836	0.9990	-1.27	not estimable	3.162	55.49	96.58
F1	3 / 4 / 6	711.7297	0.9907	-2.85	not estimable	0.969	40.53	168.11
F2	5 / 6 / 6	646.7601	0.9944	-2.81	not estimable	0.982	39.00	202.83
F3	3 / 6 / 6	839.6475	0.9923	-2.92	not estimable	1.018	38.74	208.08
F4	3 / 4 / 4	124.1278	0.9960	-2.09	4.77e+1 – 2.69e+2	1.401	34.99	114.33
F5	5 / 4 / 6	996.7422	0.9912	-3.00	not estimable	1.113	42.59	245.09
F6	5 / 4 / 4	1.057e+3	0.9926	-3.02	not estimable	0.804	37.50	186.71
F7	5 / 6 / 4	157.0514	0.9982	-2.20	7.02e+1 – 2.85e+2	1.351	36.27	121.70
F8	3 / 6 / 4	159.3957	0.9983	-2.20	7.21e+1 – 3.35e+2	1.378	38.27	125.50

Note: A = *A. paniculata*, T = *T. cordifolia*, C = *C. longa*. Each concentration was measured in duplicate technical wells within one assay run. Apparent IC_{50} values were calculated from the mean duplicate response. No independent assay replicates were performed; therefore, SD values reflect intra-assay technical variation only, and no ANOVA, post-hoc multiple comparisons, or p-values were reported; the 95% CIs reflect curve-fitting uncertainty only. $pIC_{50} = -\log_{10}(IC_{50}$, µg/mL). [a] For all formulations, IC_{50} > 100 µg/mL (highest tested concentration); the values shown were extrapolated from unconstrained fits whose upper asymptotes exceeded 100% and are reported for descriptive ranking only, not as reliable potency estimates.

formulations (**Table 12**), reflecting the limited coverage of the upper part of the concentration–response curves. Because the upper plateau was not captured, the top asymptote, and therefore the IC_{50}, was not adequately constrained by the data, and reliable IC_{50} values for the formulations can be obtained only by testing an expanded concentration range.

The fitted curves showed high R^2 values, ranging from 0.9907 to 0.9990. However, R^2 was interpreted together with the Hill slope, asymptotic parameters, confidence intervals, and curve diagnostics. The Hill slope values ranged from 0.804 to 1.401, indicating differences in the steepness of the concentration–response transitions. F4 showed the steepest fitted response among the formulations, whereas F6 showed the shallowest response.

The 95% confidence intervals were estimable only for F4, F7, and F8 and were relatively broad: 47.7–269, 70.2–285, and 72.1–335 µg/mL, respectively. The overlap among these intervals indicates that the apparent potency differences among F4, F7, and F8 should not be interpreted as statistically significant without formal curve-comparison analysis. For the remaining samples, the 95% confidence intervals were not estimable under the selected fitting conditions. Therefore, the IC_{50} ranking should be considered descriptive and preliminary.

The positive control (ascorbic acid) exhibited an IC_{50} of 18.48 µg/mL. Among the tested formulations, F4 showed the lowest apparent (extrapolated) IC_{50}, followed by F7 and F8. F1, F2, F3, F5, and F6 also exhibited concentration-dependent NO-scavenging activity, with their apparent IC_{50} estimates presented in **Table 12**. The differences in IC_{50} values should be interpreted alongside their confidence intervals, as overlapping intervals may indicate uncertainty in distinguishing the apparent NO-scavenging activities of the formulations. Overall, ascorbic acid exhibited greater apparent NO-scavenging activity than the tested formulations under the experimental conditions.

Reported NO-scavenging IC_{50} values for single and multiple extracts vary widely. *C. longa* rhizome extracts showed IC_{50} values of 52.5–54.3 µg/mL in the SNP assay (42). Among multi-herb products, the polyherbal formulation Rumalaya Forte, which contains *T. cordifolia* extract, exhibited an IC_{50} of 10.37 µg/mL (43). The extrapolated IC_{50} of F4 is therefore higher than those reported for the *C. longa* extract and the polyherbal product. These comparisons should be made with caution because the cited studies tested extracts or powdered products dissolved directly in the assay medium, whereas the present values were obtained from PBS dispersions of a complete emulgel and were expressed relative to its total extract content. The emulgel matrix, incomplete release of lipophilic constituents such as curcuminoids and piperine into the aqueous test medium, and removal of the oil phase during centrifugation would all be expected to lower the apparent activity relative to that of free extracts.

Ascorbic acid was used as a reference antioxidant in the sodium nitroprusside (SNP)–Griess assay because the assay evaluates the ability of the tested formulations to scavenge nitric oxide (NO) generated under cell-free conditions. Accordingly, ascorbic acid was not considered a mechanistic anti-inflammatory reference or an inhibitor of inducible nitric oxide synthase (iNOS). Its role in the present study was limited to providing a benchmark for the NO-scavenging capacity of the formulations. Further comparison with established anti-inflammatory or iNOS-targeting compounds would be more appropriate in future cell-based studies designed to investigate cellular inflammatory pathways (44).

The sodium nitroprusside (SNP)–Griess assay was employed as an initial cell-free screening method to assess

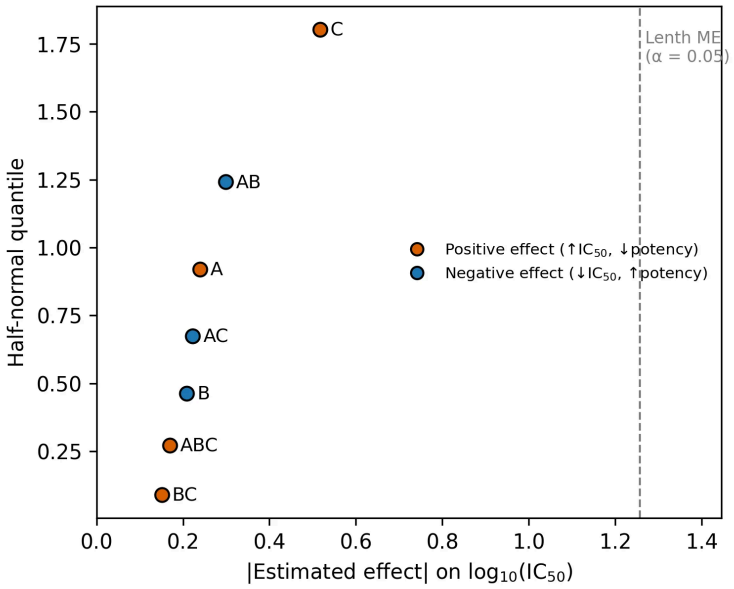


Figure 3. Half-normal plot of the estimated factorial effects on $\log_{10}(IC_{50})$ for NO scavenging. A = *A. paniculata*, B = *T. cordifolia*, C = *C. longa*. Orange symbols indicate positive effects (higher IC_{50}, lower potency) and blue symbols indicate negative effects. The dashed line indicates Lenth's margin of error (α = 0.05).

the NO-scavenging potential of the formulated emulgels. Although NO is an important mediator of inflammatory processes and may contribute to vascular changes associated with topical steroid withdrawal (TSW), the present assay does not provide direct evidence of inhibition of cellular inflammatory pathways or iNOS-mediated NO production (45). Accordingly, these findings provide preliminary evidence of the NO-scavenging capacity of the formulations but do not establish their direct anti-inflammatory efficacy in the context of TSW (46).

It should be emphasized that, in this assay, NO is released non-enzymatically from SNP in a buffered, cell-free medium. No cells, NO synthase, or inflammatory stimulus are present in the reaction system; therefore, the decrease in nitrite observed in the presence of the emulgel samples can result only from direct chemical scavenging of NO, or of NO-derived reactive nitrogen species, by constituents released from the formulation. The present data thus demonstrate direct NO-scavenging capacity, and they do not demonstrate cellular anti-inflammatory efficacy, suppression of cellular NO production, or direct inhibition of iNOS activity or expression. Although andrographolide, *T. cordifolia* constituents, and curcuminoids have been reported to down-regulate iNOS, COX-2, and related inflammatory mediators in cellular and animal models (8, 11, 12), such effects were not evaluated in the present study and cannot be inferred from these results. Moreover, direct NO scavenging in a chemical system does not necessarily translate into an anti-inflammatory effect in the skin, where NO availability depends on enzymatic NO production, cellular redox status, and the penetration of active constituents into the tissue. Demonstrating anti-inflammatory relevance will therefore require cell-based models in which NO is produced enzymatically, such as LPS-stimulated macrophages or keratinocytes, with concurrent cell-viability testing and measurement of nitrite, iNOS expression, and pro-inflammatory cytokines, followed by in vivo evaluation.

Effect of Formulation Variables on NO-Scavenging Potency

The 2^3 full factorial design was used to evaluate how the three variable extracts influenced NO-scavenging potency. Because the IC_{50} values spanned almost one order of magnitude (124–1,057 µg/mL), the response was analysed as $\log_{10}(IC_{50})$. The coded polynomial model obtained from the eight formulations is given in **Equation 3**, where X_1, X_2, and X_3 are the coded levels of *A. paniculata* (3–5%), *T. cordifolia* (4–6%), and *C. longa* (4–6%), respectively. Positive coefficients indicate an increase in IC_{50} (lower NO-scavenging potency), whereas negative coefficients indicate a decrease in IC_{50} (higher potency). Because the design was unreplicated and the model is saturated, **Equation 3** reproduces the eight observed formulations exactly and has no residual degrees of freedom; it should therefore be used to interpret the direction and relative magnitude of the effects rather than to predict untested formulations. In addition, because the response variable was derived from IC_{50} values extrapolated beyond the tested concentration range, the factorial effects describe the pattern of these apparent estimates only; they should be regarded as hypothesis-generating and re-estimated

$$\log_{10}(\mathrm{IC}_{50}) = 2.638 + 0.120X_1 - 0.104X_2 + 0.259X_3 - 0.150X_1X_2 - 0.111X_1X_3 + 0.075X_2X_3 + 0.085X_1X_2X_3 \quad \textbf{(Eq. 3)}$$

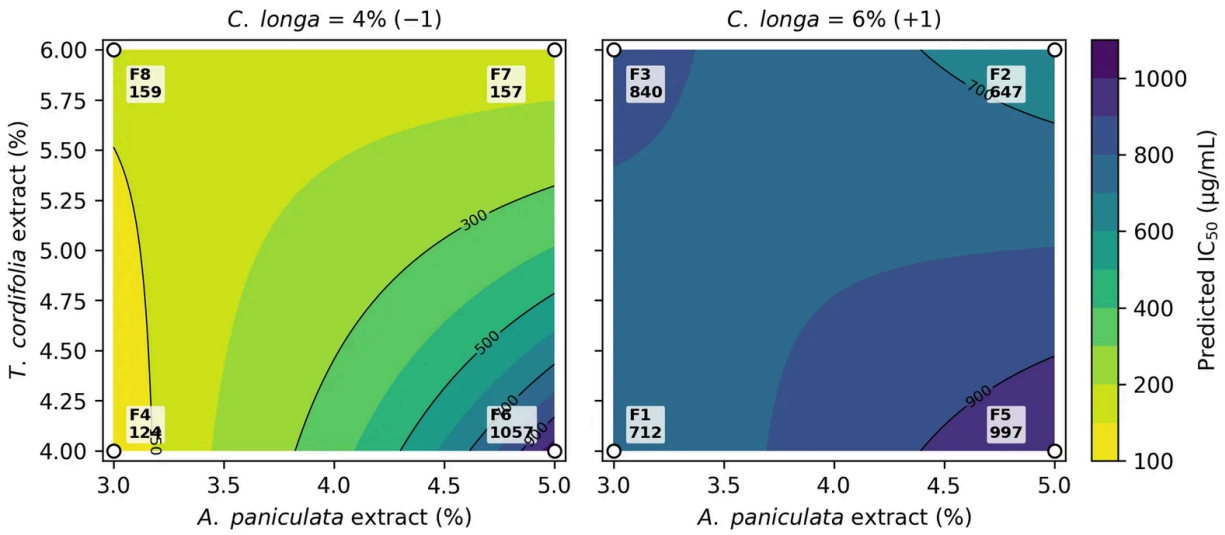


Figure 4. Contour plots of predicted IC_{50} (µg/mL) as a function of *A. paniculata* and *T. cordifolia* concentrations at 4% (left) and 6% (right) *C. longa*, derived from Equation (3). Symbols indicate the experimental formulations and their observed IC_{50} values.

once IC_{50} values are determined within an expanded concentration range.

The half-normal plot (**Figure 3**) showed that the *C. longa* main effect (X_3) was the largest, accounting for approximately 48% of the total variation in $\log_{10}(IC_{50})$, followed by the *A. paniculata* × *T. cordifolia* interaction (X_1X_2; 16%), the *A. paniculata* main effect (X_1; 10%), the X_1X_3 interaction (9%), and the *T. cordifolia* main effect (X_2; 8%). The Shapiro–Wilk test of the effect estimates ($W = 0.910$, $p = 0.393$) did not indicate a departure from normality; however, none of the effects exceeded Lenth's margin of error (1.26 log units, $\alpha = 0.05$), so the effects cannot be declared statistically significant with the present unreplicated data.

Despite this limitation, the pattern of effects is informative for formulation development (**Figure 4**). Increasing *C. longa* from 4% to 6% increased $\log_{10}(IC_{50})$ by 0.52 units on average, corresponding to an approximately 3.3-fold increase in IC_{50}, and all four formulations containing 6% *C. longa* (F1, F2, F3, and F5) had IC_{50} values above 640 µg/mL. At 4% *C. longa*, the effect of *A. paniculata* depended strongly on the level of *T. cordifolia* (X_1X_2 interaction): increasing *A. paniculata* from 3% to 5% raised the IC_{50} approximately 8.5-fold when *T. cordifolia* was 4% (F4 vs F6; 124 vs 1,057 µg/mL) but had almost no effect when *T. cordifolia* was 6% (F8 vs F7; 159 vs 157 µg/mL). Thus, the most active formulations were the one with the lowest total extract loading (F4) and those combining low *C. longa* with balanced levels of *A. paniculata* and *T. cordifolia* (F7 and F8), indicating that NO-scavenging potency was not additive with respect to extract concentration.

Several factors may explain this less-than-additive behaviour. Because sample concentrations were normalized to total extract content, formulations with a higher *C. longa* loading contained a larger proportion of curcuminoids, which are poorly water-soluble and are likely to partition into the oil phase and to be partly removed during centrifugation of the PBS dispersion. Higher extract loading may also increase interactions between phenolic constituents and the Carbopol–surfactant matrix, limiting their release into the aqueous test medium. Antagonistic chemical interactions among the extract constituents, which have been reported for some phytochemical mixtures (7, 23), cannot be excluded. These explanations are hypotheses that were not tested directly and should be examined in future release and solubility studies. Nevertheless, within these constraints, the factorial analysis supports the provisional selection of F4 as the lead formulation and suggests that further optimization should explore lower *C. longa* levels rather than higher overall extract loading.

Limitations of the Study

This study has several limitations. First, antioxidant activity was evaluated using a cell-free nitric oxide-scavenging assay based on the sodium nitroprusside (SNP)–Griess method. Although this assay measures the chemical inhibition of nitrite formation, it does not directly establish intracellular antioxidant activity, enzymatic NO-synthase inhibition, or in vivo anti-inflammatory efficacy. The assay may also be affected by reaction conditions and matrix-related spectral or chemical interference from co-extracted constituents. In addition, the assay does not capture the complexity of cellular responses or biological processes involved in inflammation. Thus, the IC_{50} values should be interpreted within the scope of the assay as indicators of apparent NO-scavenging capacity, while further studies using biologically relevant models are needed to establish the biological significance of these findings (46).

Second, and most importantly, the assay was performed using duplicate technical wells in a single experimental run. These duplicate measurements provide an indication of within-run measurement repeatability but do not represent independent experimental replicates. Consequently, between-run variability could not be estimated, and confidence intervals for the IC_{50} values, ANOVA-based inference, or formal multiple comparisons

among formulations could not be reliably performed. The reported NO-scavenging results and formulation ranking should therefore be considered strictly preliminary and descriptive. The same limitation prevented formal significance testing of the factorial effects, which were therefore interpreted as exploratory. Independent assay runs conducted on at least three separate occasions, preferably with triplicate technical wells at each concentration, are required to validate these findings before any conclusion on relative potency can be drawn (44).

Third, the present study did not assess cellular uptake, intracellular metabolism, cytotoxicity, or the effects of the extracts on the iNOS pathway. Therefore, the results cannot distinguish direct chemical NO scavenging from inhibition of enzymatic NO production. Further studies should combine the cell-free assay with cell-based inflammatory models, such as LPS-stimulated macrophages, together with cell-viability testing and measurement of NO, iNOS, and relevant inflammatory mediators. Such models would provide complementary evidence regarding the biological relevance of the observed activity but should not be considered directly equivalent to the present cell-free chemical assay because they involve additional cellular and molecular processes (47).

Fourth, the IC_{50} values of all formulations exceeded the highest concentration tested (100 µg/mL) and were obtained by extrapolation of unconstrained four-parameter logistic fits. Because the upper plateau of the concentration–response curve was not captured, the formulation IC_{50} values are reported as > 100 µg/mL, and the extrapolated estimates were used only descriptively. In the planned validation study, the tested range will be expanded (for example, to approximately 1,000–2,000 µg/mL, or until a clear upper plateau is observed), with additional concentrations around the expected IC_{50}, more concentrated stock dispersions where necessary, and appropriate sample blanks to correct for matrix colour and turbidity. This will allow IC_{50} values to be determined by interpolation within the experimental range, the top asymptote to be constrained to 100%, and the factorial analysis to be repeated on reliable IC_{50} values.

Fifth, the physical evaluation was limited to the parameters reported here. Extrudability, rheological profiling, and accelerated and long-term stability testing (e.g., heating–cooling cycles and storage at different temperatures) were not performed, so the shelf life and in-use performance of the emulgels remain to be established. Finally, the four botanicals were selected on the basis of their ethnomedicinal use, published pharmacological evidence, and our previous spray-gel study (11) rather than by in silico screening, and no cell-line or animal studies were conducted. Molecular docking or network-pharmacology analysis, cell-based assays, in vivo anti-inflammatory models, and stability studies are planned for the lead formulation F4.

The main focus of this study was to compare the NO-scavenging potential of the formulated emulgels. The physical evaluation was conducted primarily to characterize the physical properties of the prepared formulations and to provide supplementary information on their formulation characteristics. Accordingly, these physical parameters were not considered primary comparative outcomes and were therefore not subjected to statistical analysis.

Conclusion

A multi-extract emulgel containing *A. paniculata*, *T. cordifolia*, *C. longa*, and *P. nigrum* was successfully formulated in eight variants using a 2^3 full factorial design. All formulations were homogeneous oil-in-water systems with skin-compatible pH (5.26–5.90) and viscosity (12,560–17,120 cP), indicating acceptable physical characteristics for topical application. In the cell-free sodium nitroprusside–Griess assay, nitrite reduction increased consistently with concentration over 20–100 µg/mL ($R^2 \geq 0.990$). However, the IC_{50} values of all formulations exceeded the highest tested concentration and are reported as > 100 µg/mL; extrapolated estimates ranked F4 first, followed by F7 and F8, but their 95% confidence intervals were broad and overlapping and were not estimable for the remaining formulations, so the potency ranking is descriptive rather than statistically established. Exploratory factorial analysis of these estimates suggested that *C. longa* concentration and the *A. paniculata* × *T. cordifolia* interaction were the main contributors to the variation in IC_{50} and that higher extract loading did not improve NO-scavenging potency. Accordingly, the findings support only direct chemical scavenging of nitric oxide under cell-free conditions and do not demonstrate inhibition of cellular NO production, iNOS expression, or anti-inflammatory efficacy relevant to topical steroid withdrawal. All NO-scavenging findings are therefore strictly preliminary and descriptive and require validation through independent assay runs on at least three separate occasions, using an expanded concentration range that captures the complete upper plateau of the concentration–response curve. F4 is provisionally proposed as the lead candidate for this confirmatory testing and for subsequent cell-based studies, including LPS-stimulated macrophage models with cytotoxicity testing and measurement of NO, iNOS, and related inflammatory mediators, followed by stability testing and in vivo anti-inflammatory evaluation.

Abbreviations

AD = Atopic Dermatitis; COX-2 = Cyclooxygenase-2; DMDM hydantoin = Dimethylol Dimethyl Hydantoin; IC_{50} = Half-Maximal Inhibitory Concentration; iNOS = Inducible Nitric Oxide Synthase; LPS = Lipopolysaccharide; MAPK = Mitogen-Activated Protein Kinase; NF-κB = Nuclear Factor-kappa B; NO = Nitric Oxide; NSAID = Non-Steroidal Anti-Inflammatory Drug; O/W = Oil-in-Water; PBS = Phosphate-Buffered Saline; PGE2 = Prostaglandin E2; SNP = Sodium Nitroprusside; TCS = Topical Corticosteroid; TEA = Triethanolamine; TSW = Topical Steroid Withdrawal.

Declaration

Author Information

Wahyu Bachtiar *(*Corresponding author)*, Department of Pharmacy, STIKes Widya Dharma Husada Tangerang, South Tangerang, Indonesia. **Contribution:** Conceptualization.

Tyssa Mariyana, Department of Pharmacy, STIKes Widya

Dharma Husada Tangerang, South Tangerang, Indonesia. **Contribution:** Data Curation .

Nurul Hidayatri, Department of Pharmacy, STIKes Widya Dharma Husada Tangerang, South Tangerang, Indonesia. **Contribution:** Formal Analysis.

Bheta Sari Dewi, Department of Pharmacy, STIKes Widya Dharma Husada Tangerang, South Tangerang, Indonesia. **Contribution:** Writing – Original Draft.

Ayu Werawati, Department of Pharmacy, STIKes Widya Dharma Husada Tangerang, South Tangerang, Indonesia. **Contribution:** Validation.

Acknowledgment
The authors would like to express their sincere gratitude to the Ministry of Higher Education, Science, and Technology (Kemdiktisaintek) of the Republic of Indonesia for the financial support provided through the 2026 Beginner Lecturer Research Grant (Penelitian Dosen Pemula/PDP), under Grant Agreement No. 283/C3/DT.05.00/PL-BARU/2026. During this study and the preparation of the manuscript, the authors used Claude (Anthropic, USA) to help understand the methodology, edit the English, analyse the factorial design, and check references. AI was not used to generate or alter the experimental data. All AI-assisted output was reviewed and verified by the authors, who take full responsibility for the content of this article.

Conflict of Interest
The authors declare no conflict of interest.

Data Availability
All data generated or analyzed during this study are included in this published article and its supplementary information files.

Ethics Statement
Not applicable.

Funding Information
This work was funded by Kemendiktisaintek under grant number 283/C3/DT.05.00/PL-BARU/2026.

References
1. Choi H, Orbe M, Esam S, Parker J. An Updated Systematic Review of Topical Corticosteroid Withdrawal (TCSW): Steroid Addiction or Adverse Drug Effect?. Cureus. 2026;8(4):1-12. doi: https://doi.org/10.7759/cureus.107365

2. Hsu C, Guo L, Adams D, Davis D, Eichenfield L, Hsu Friedman O, *et al*. Topical steroid withdrawal syndrome: developing diagnostic criteria through a modified Delphi method. British Journal of Dermatology. 2025;194(4):768-778. doi: https://doi.org/10.1093/bjd/ljaf518

3. Orr N, Rogers M, Stein A, Thompson Coon J, Stein K. Reviewing the Evidence Base for Topical Steroid Withdrawal Syndrome in the Research Literature and Social Media Platforms: An Evidence Gap Map. J Med Internet Res. 2024;26:e57687. doi: https://doi.org/10.2196/57687

4. Alsterholm M, Af Klinteberg M, Vrang S, Sigurdardottir G, Sandström Falk M, Shayesteh A. Topical Steroid Withdrawal in Atopic Dermatitis: Patient-reported Characterization from a Swedish Social Media Questionnaire. Acta Derm Venereol. 2025;105:adv40187. doi: https://doi.org/10.2340/actadv.v105.40187

5. Chen X, Ren J, Yang J, Zhu Z, Chen R, Zhang L. A critical review of *Andrographis paniculata*. Mpb. 2023;2(1):0-0. doi: https://doi.org/10.48130/mpb-2023-0015

6. Li X, Yuan W, Wu J, Zhen J, Sun Q, Yu M. Andrographolide, a natural anti-inflammatory agent: An Update. Front. Pharmacol. 2022;13:920435. doi: https://doi.org/10.3389/fphar.2022.920435

7. Bharathi Priya L, Balasubramanian B, Shanmugaraj B, Subbiah S, Hu RM, Huang CY, *et al*. Therapeutic Potential of the Medicinal Plant *Tinospora cordifolia*–Minireview. Phyton. 2022;91(6):1129-1140. doi: https://doi.org/10.32604/phyton.2022.017707

8. Pasha A, Kumar K, Heena SK, Arnold Emerson I, Pawar SC. Inhibition of NF-kB and COX-2 by andrographolide regulates the progression of cervical cancer by promoting PTEN expression and suppressing PI3K/AKT signalling pathway. Sci Rep. 2024;14(1):1-22. doi: https://doi.org/10.1038/s41598-024-57304-7

9. Adri TA, Wulandari T, Mansyur M. Uji efek antiinflamasi dan analgetik ekstrak etanol daun jati putih (*Gmelina arborea* Roxb) pada mencit jantan (Mus musculus). Teknosains: Media Informasi Sains dan Teknol. 2025;19(3):354-364. doi: https://doi.org/10.24252/teknosains.v19i3.60727

10. Mus NM, Prasetya F, Widowati L, Bafadal M, Nisaa NR, Isnawati A. Anti-Inflammatory Activity of Dysmenorrhea Herbal Medicine Through Inhibition of the Cyclooxygenase Enzyme and Identification of Compound in Sambiloto Extract. Indonesian Journal of Pharmaceutical Science and Technology. 2024 Jul 31;6(1):18-26. https://jurnal.unpad.ac.id/ijpst/article/view/53219

11. Bachtiar W, Sari Dewi B, Werawati A. Inovasi Spray Gel Kombinasi Sambiloto, Brotowali, Kunyit, Dan Lada Hitam Sebagai Alternatif Non-Steroid Untuk Pemulihan Eksim Topical Steroid Withdrawal. Edu Masda Journal. 2025 Sep 2;9(2):125–37. https://openjournal.masda.ac.id/index.php/edumasda/article/view/277

12. Permatasari I, Jasaputra DK, Windi J, Anania A. Pengaruh Emulgel Ekstrak Kunyit (*Curcuma longa*) terhadap Ekspresi Gen Tumor Nekrosis Alpha (Tnf- A) dan Densitas Kolagen pada Tikus Galur Wistar Jantan (*Rattus norvegicus*) yang Dipapar Sinar Ultraviolet B (Uvb). Jurnal sostech. 2026;6(1):251-263. doi: https://doi.org/10.59188/jurnalsostech.v6i1.32660

13. Dinul Hikmah F, Ahwan A. Formulasi dan Evaluasi Sediaan Tablet Antiinflamasi Kombinasi Ekstrak Kunyit (*Curcuma longa* L) dan Jahe (*Zingiber officinale*). Farmestra. 2026;3(02):79-90. doi: https://doi.org/10.66340/43hbpq30

14. Man MQ, Wakefield JS, Mauro TM, Elias PM. Regulatory Role of Nitric Oxide in Cutaneous Inflammation. Inflammation. 2022 Jun 1;45(3):949–64. doi:10.1007/s10753-021-01615-8

15. Zaborova V, Budanova E, Kryuchkova K, Rybakov V, Shestakov D, Isaikin A, *et al*. Nitric oxide: a gas transmitter in healthy and diseased skin. Medical Gas Research. 2025;15(4):520-528. doi: https://doi.org/10.4103/mgr.medgasres-d-24-00144

16. Huang X, Li Y, Sabier M, Si J, Wang P, Shen Y, *et al*. Guidelines for the *in vitro* determination of anti-inflammatory activity. eFood. 2024;5(3). doi: https://doi.org/10.1002/efd2.160

17. Kim ME, Lee JS. Advances in the Regulation of Inflammatory Mediators in Nitric Oxide Synthase: Implications for Disease Modulation and Therapeutic Approaches. Ijms. 2025;26(3):1204. doi: https://doi.org/10.3390/ijms26031204

18. Donthi MR, Munnangi SR, Krishna KV, Saha RN, Singhvi G, Dubey SK. Nanoemulgel: A Novel Nano Carrier as a Tool for Topical Drug Delivery. Pharmaceutics. 2023;15(1):164. doi: https://doi.org/10.3390/pharmaceutics15010164

19. 19. Mahyoob Alburyhi M, Alwan Noman M, Ahmed Saif A, Abd-hafiz Al-Ghorafi M, Al Khawlani MA, A Yahya TA, et al. Formulation And Evaluation Of Anti-Acne Spironolactone Emulgel Novel Trend In Topical Drug Delivery System. World J Pharm Res. 2023;12(22):96–119. doi:10.20959/wjpr202322-30742

20. 20. Milutinov J, Krstonošić V, Ćirin D, Pavlović N. Emulgels: Promising Carrier Systems for Food Ingredients and Drugs. Polymers. 2023;15(10):2302. doi:10.3390/polym15102302

21. Yılmaz Usta D, Teksin ZS, Tugcu-Demiroz F. Evaluation of Emulgel and Nanostructured Lipid Carrier-Based Gel Formulations for Transdermal Administration of Ibuprofen: Characterization, Mechanical Properties, and *Ex-Vivo* Skin Permeation. AAPS PharmSciTech. 2024;25(5). doi: https://doi.org/10.1208/s12249-024-02831-9

22. Kassab HJ, Alkufi HK, Hussein LS. Use of factorial design in formulation and evaluation of intrarectal *in situ* gel of sumatriptan. Journal of Advanced Pharmaceutical Technology & Research. 2023;14(2):119-124. doi: https://doi.org/10.4103/japtr.japtr_603_22

23. Wink M. Current Understanding of Modes of Action of Multicomponent Bioactive Phytochemicals: Potential for Nutraceuticals and Antimicrobials. Annu. Rev. Food Sci. Technol. 2022;13(1):337-359. doi: https://doi.org/10.1146/annurev-food-052720-100326

24. Yang EJ, Yim EY, Song G, Kim GO, Hyun CG. Inhibition of nitric oxide production in lipopolysaccharide-activated RAW 264.7 macrophages by Jeju plant extracts. Interdisciplinary Toxicology. 2009;2(4):245-249. doi: https://doi.org/10.2478/v10102-009-0022-2

25. Dugganaboyana GK, Kumar Mukunda C, Jain A, Kantharaju RM, Nithya RR, Ninganna D, *et al*. Environmentally benign silver bio-nanomaterials as potent antioxidant, antibacterial, and antidiabetic agents: Green synthesis using *Salacia oblonga* root extract. Front. Chem. 2023;11. doi: https://doi.org/10.3389/fchem.2023.1114109

26. Liu W, Song W, Luo Y, Dan H, Li L, Zhang Z, *et al*. Angelica Yinzi alleviates 1-chloro-2,4-dinitrobenzene-induced atopic dermatitis by inhibiting activation of NLRP3 inflammasome and down-regulating the MAPKs/NF-kB signaling pathway. Saudi Pharmaceutical Journal. 2022;30(10):1426-1434. doi: https://doi.org/10.1016/j.jsps.2022.07.003

27. Sari Dewi B, Meitania Utami S, Season Alamsyah S, Tri Rahmadani N. Formulation and Antioxidant Activity of Syrup Preparation Containing Saga Leaf Extract (*Abrus precatorius* L.). Jurnal Kefarmasian Indonesia. 2025 Feb 28;15(1):70–9. doi:10.22435/jki.v15i1.6695

28. Jariah A, Hadisaputra S, Purwoko AA. Characterization of M-curcumin complexes (M= Cu, Co, Ag) in turmeric rhizome as sensitizer candidates in dye-sensitized solar cell (DSSC). Acta.Chim.Asiana. 2023;6(1):287-294. doi: https://doi.org/10.29303/aca.v6i1.152

29. Octavia MD, Zaini E, Hasmiwati H, Revila G. ISOLASI PIPERIN DARI LADA HITAM (*Piper nigrum* L.) DAN UJI KEMURNIANNYA. Higea. 2024;16(1):52. doi: https://doi.org/10.52689/higea.v16i1.621

30. Rohana E, Ekawati N, Hapsari II. Development and validation of a dissolution test for andrographolide dispersible tablets using UV-Vis spectrophotometry. Pharm Educ. 2024;24(6):28-34. doi: https://doi.org/10.46542/pe.2024.246.2834

31. Rauf J, Isa I, Thomas NA. Formulasi Sediaan Emulgel Ekstrak Daun Kelor (*Moringa oleifera* Lam) Dan Uji Aktivitas Antioksidan Menggunakan Metode DPPh. Ijpe. 2021;1(1):10-19. doi: https://doi.org/10.37311/ijpe.v1i1.9947

32. Zam Zam AN, Musdalifah M. Formulasi dan Evaluasi Kestabilan Fisik Krim Ekstrak Biji Lada Hitam (*Piper nigrum* L.) Menggunakan Variasi Emulgator. Jsscr. 2022;4(2):304-313. doi: https://doi.org/10.37311/jsscr.v4i2.14146

33. Chitiva LC, Santamaría-Torres MA, Rezende-Teixeira P, Borlot JRPDO, Romagna RDA, Londoño X, *et al*. Uncovering Metabolic Alterations in HCT-116 Colon Cancer Cells upon Exposure to Bamboo Leaf Extract Obtained from *Guadua incana* Londoño. Molecules. 2024;29(13):2985. doi: https://doi.org/10.3390/molecules29132985

34. Wulandari R, Monica E, Yoedistira CD. Formulasi Dan Uji Mutu Fisik Krim Anti Aging Yang Mengandung Ekstrak Labu Kuning (*Cucurbita moschata* Duch). Sainsbertek Jurnal Ilmiah Sains & Teknologi. 2022;3(1):248–56. https://doi.org/10.33479/sb.v3i1.182

35. Af N, Anas idah, Subhiaty Idrus L, Wibawa Mahatva Yodha A. Studi In Vitro: Potensi Antiinflamasi Ekstrak Rimpang Tanaman Wundu Watu (*Alpinia monopleura*) Melalui Penghambatan Nitric Oxide. J Sains dan Teknologi Pangan. 2025 Sep 8;10(5):8855–62. https://jstpuho.id/index.php/jstp/article/view/172

36. Dewi BS, Surini S. Study on hydrogel eye mask with *Centella asiatica* L and *Aloe vera* L extract. J Adv Pharm Educ Res. 2024;14(2):27-34. doi: https://doi.org/10.51847/9utowxppyp

37. Anggraini H. Formulasi dan uji stabilitas fisik gel hand sanitizer kombinasi ekstrak daun sirih hijau (*Piper betle*) dan ekstrak daun kelor (*M. oleifera*) sebagai antimikroba. Jptb. 2022;1(1):38-49. doi: https://doi.org/10.62619/jptb.v1i1.83

38. Adawiyah R, Ridho R. Formulasi, uji stabilitas sediaan gel ekstrak etanol daun stroberi (*Fragaria x ananassa*) dan uji aktivitas antibakteri *Propionibacterium acnes* penyebab jerawat. jff. 2024;2(1):23-38. doi: https://doi.org/10.35760/jff.2024.v2i1.9705

39. Bakri A, Sinala S, Ratnah S. Formulasi Emulgel Ekstrak Ubi Jalar Ungu (*Ipomoea batatas* (L.) Poiret) dengan Variasi Gelling Agent. Jurnal Mandala Pharmacon Indonesia (JMPI). 2023 Jun 30;9(1):1–9. https://jurnal-pharmaconmw.com/jmpi/index.php/jmpi/article/view/201/107

40. Thongphichai W, Hasriadi H, Wasana PWD, Jayashan SS, Sritularak B, Towiwat P, *et al.* Anti-inflammatory activity of *Curcuma wanenlueanga* Saensouk, Thomudtha & Boonma rhizomes and the search for its bioactive markers by harmonizing bioassay-guided isolation and network pharmacology. BMC Complement Med Ther. 2025;25(1). doi: https://doi.org/10.1186/s12906-025-04884-0

41. Charoenphun N, Klangbud WK. Antioxidant and anti-inflammatory activities of durian (*Durio zibethinus*Murr.) pulp, seed and peel flour. PeerJ. 2022;10:e12933. doi: https://doi.org/10.7717/peerj.12933

42. Quirós-Fallas MI, Vargas-Huertas F, Quesada-Mora S, Azofeifa-Cordero G, Wilhelm-Romero K, Vásquez-Castro F, *et al.* Polyphenolic HRMS Characterization, Contents and Antioxidant Activity of *Curcuma longa* Rhizomes from Costa Rica. Antioxidants. 2022;11(4):620. doi: https://doi.org/10.3390/antiox11040620

43. Subash KR, Somasundaram G, Jagan Rao N, Muthulakshmi Bhaarati G, Cheriyan BV, Sandeep Kumar K. Studies on the *in vitro* anti-oxidant properties of a polyherbal formulation: Rumalaya Forte. J Clin Diagn Res. 2012;6(7):1254–7. doi:10.7860/JCDR/2012/4489.2431

44. Hassan HHAM, Hussien H, Elhusseiny AF. Green synthesis of nanosized N,N′-bis(1-naphthylidene)-4,4′-diaminodiphenylmethane and its metal (II) complexes and evaluation of their biological activity. Sci Rep. 2022 Dec 1;12(1):1–19. doi:10.1038/s41598-022-25650-z

45. Iqbal MO, Gu Y, Khan IA, Wang R, Chen J. Evaluation of the *in vitro* antioxidant and antitumor activity of hydroalcoholic extract from *Jatropha mollissima* leaves in Wistar rats. Front. Chem. 2023;11. doi: https://doi.org/10.3389/fchem.2023.1283618

46. Cañas S, Rebollo-Hernanz M, Bermúdez-Gómez P, Rodríguez-Rodríguez P, Braojos C, Gil-Ramírez A, *et al.* Radical Scavenging and Cellular Antioxidant Activity of the Cocoa Shell Phenolic Compounds after Simulated Digestion. Antioxidants. 2023;12(5):1007. doi: https://doi.org/10.3390/antiox12051007

47. Xu H, Liu M, Chen G, Wu Y, Xie L, Han X, *et al.* Anti-Inflammatory Effects of Ginsenoside Rb3 in LPS-Induced Macrophages Through Direct Inhibition of TLR4 Signaling Pathway. Front. Pharmacol. 2022;13. doi: https://doi.org/10.3389/fphar.2022.714554

Additional Information

How to Cite

APA 7th Edition: Bachtiar, W., Mariyana, T., Hidayatri, N., Dewi, B. S. & Werawati, A. (2026). Griess Assay Evaluation of Nitric Oxide Scavenging by a Multi-Extract Emulgel for Topical Steroid Withdrawal. Sciences of Pharmacy, 5(4), 410-425. https://doi.org/10.58920/sciphar0504785

Vancouver: Bachtiar W, Mariyana T, Hidayatri N, Dewi BS, Werawati A. Griess Assay Evaluation of Nitric Oxide Scavenging by a Multi-Extract Emulgel for Topical Steroid Withdrawal. Sciences of Pharmacy. 2026;5(4):410-425. https://doi.org/10.58920/sciphar0504785

Harvard: Bachtiar, W., Mariyana, T., Hidayatri, N., Dewi, B. S. & Werawati, A. (2026) 'Griess Assay Evaluation of Nitric Oxide Scavenging by a Multi-Extract Emulgel for Topical Steroid Withdrawal', Sciences of Pharmacy, 5(4), pp. 410-425. doi: 10.58920/sciphar0504785

Publisher Note

All claims expressed in this article are solely those of the authors and do not necessarily reflect the views of the publisher, the editors, or the reviewers. Any product that may be evaluated in this article, or claim made by its manufacturer, is not guaranteed or endorsed by the publisher. The publisher remains neutral with regard to jurisdictional claims in published maps and institutional affiliations.

Open Access

This article is licensed under a Creative Commons Attribution 4.0 International License. You may share and adapt the material with proper credit to the original author(s) and source, include a link to the license, and indicate if changes were made.